Geothermal Driven micro-CCHP for Domestic Application - Exergy, Economic and Sustainability Analysis

Nami, Hossein; Anvari-Moghaddam, Amjad

Published in:
Energy

DOI (link to publication from Publisher):
10.1016/j.energy.2020.118195

Publication date:
2020

Document Version
Accepted author manuscript, peer reviewed version

Citation for published version (APA):
Nami, H., & Anvari-Moghaddam, A. (2020). Geothermal Driven micro-CCHP for Domestic Application - Exergy, Economic and Sustainability Analysis. *Energy*, *207*, 1-16. Article 118195.
https://doi.org/10.1016/j.energy.2020.118195

Geothermal Driven micro-CCHP for Domestic Application – Exergy, Economic and Sustainability Analysis

Hossein Nami[a,*], Amjad Anvari-Moghaddam[b,c]

[a] Department of Mechanical Engineering, Faculty of Engineering, University of Maragheh, P.O.Box 83111-55181, Maragheh, Iran

[b] Department of Energy Technology, Aalborg University, 9220 Aalborg East, Denmark

[c] Faculty of Electrical and Computer Engineering, University of Tabriz, Tabriz, Iran

[*]Email: h.nami@maragheh.ac.ir

Abstract

Geothermal energy is going to play a key role in future smart energy systems. Geothermal-driven domestic energy systems, specifically, will largely contribute to the baseload supply of heating and cooling demand of societies. A low-temperature geothermal resource is considered to drive a domestic-scaled multi-generation system supplying power, heating, and cooling. The proposed cogeneration system includes a small-scale organic Rankine cycle (ORC), a single effect LiBr-H_2O absorption chiller, and heat exchangers to supply domestic space heating and hot water. The waste heat of the ORC is harvested, also, to be used in space heating. Energy, exergy, economic, and sustainability principles are applied to the system to evaluate the system thermodynamic and thermos-economic performance. Results associated with the exergy destruction are obtained and effects on the system performance of chiller supply are investigated. Besides, the thermodynamic performance of the system is evaluated under the summertime and wintertime conditions. Under the base condition, the generator employed in the absorption chiller is found to be the most exergy destructive unit followed by the evaporator utilized in the ORC. Furthermore, results revealed that by increasing the chiller supply rate, the system sustainability index enhances from 1.6 to 2.5 while the system's first law efficiency reduces.

Keywords: Geothermal-Driven CCHP; Exergy; ORC; District Heating; District Cooling; Sustainability.

1. Introduction

Over the past decade, utilizing renewable resources for domestic applications has received an increasing attention. Amongst others, geothermal is a reliable, clean, and sustainable renewable energy source that has been widely used for domestic heating since 1892 in Boise, Idaho, USA [1]. Using geothermal resources for domestic heating seems to be a promising technology in Turkey as many successful projects have also reported in this regard [2]. Turkey has a considerable geothermal potential mainly due to its geographical location in the tectonically-active Alpine-Mediterranean Belt [3]. As reported by Turkey's energy agency, the geothermal potential is employed in several local sectors to the extent of 1150 MWe electricity production, and 1033 MWt direct heat generation as well as 1005 MWt in balneology, 820 MWt in greenhouse heating, 420 MWt in the hotel industry (mainly as heating), 42.8 in heat pump application and 1.5 MWt in food drying [4]. However, more attention should be paid to utilizing such energy sources in the domestic application according to Turkey's Vision 2023 energy policy. Indeed, through the widespread exploitation of geothermal resources and other types of renewables, it is possible to make a cleaner energy mix, achieve a better economy, and get higher sustainability degrees [1,5]. Besides, compared to other renewables, geothermal resources not only operate with a relatively higher capacity factor (> 80%) but also play an important role in reducing CO_2 emissions and other negative environmental footprints[6]. The following literature review presents some of the most recently published papers in the field of application of geothermal energy in the multi-generation energy systems.

Advanced exergy and exergoeconomic analysis for a cogeneration system operating in a geothermal cascade are studied by Ambriz-Díaza et al. [7]. The examined multi-generation system was able to supply the power output of 40 kWe, a cooling effect of 175.8 kWf, and 30 kWt of useful heat for dehydration. Soltani et al. [8] conducted a comprehensive review of geothermal energy evolution and development. An overview of relevant technologies at the industrial level, such as site identification, power production methods, and direct use was provided in this study. A multi-generation system was proposed by Alirahmi et al. [9] based on geothermal energy and parabolic trough solar collectors for the simultaneous generation of power, cooling, freshwater, hydrogen, and heat. It was shown that the exergy efficiency of the system could reach 29.95% under the optimum condition. Soltani et al. [10] presented a general overview of geothermal heating and cooling systems. Recognition and accommodation of several factors were addressed and discussed in that study, which could enhance the design and implementation of any geothermal heating or cooling

system. Ratlamwala et al. [11] proposed a geothermal-driven solar-boosted cogeneration system for a domestic area to supply power and district heating/cooling, while hydrogen and freshwater were produced as byproducts. A sensitivity analysis with a change in the ambient temperature, solar irradiation density, and geothermal resource condition on the system performance was performed. The examined system was capable of producing 6.776 kW power and 33.743 g per hour hydrogen with solar radiation of 1000 W/m^2. Authors in [12] suggested a new configuration of district heating system fueled with natural gas while being equipped with a deep geothermal resource. The main aim was to utilize geothermal energy in existing conventional gas-fired district heating systems to upgrade them thermodynamically and economically. Their findings showed that using geothermal sources could increase the system exergy efficiency and heating cost by about 12 and 25%, respectively, while reduce natural gas consumption by about 54%. Deployment of geothermal energy sources in Turkey was studied in [13] from sustainable development point of view. In the same study, more attention was paid to greenhouse gas emission releasing from Turkey's coal power plants. In this way, the potential of geothermal resources located in Turkey was considered in carbon capture and storage systems implementation. The optimization of parallel distribution between domestic heat and electricity supplying via geothermal energy was studied by Marty et al. [14] where a sensitivity analysis was also carried out using the source condition. Thermodynamic enhancement of the Irem binary power station located in Germencik, Turkey was performed in [15] by employing an ORC considering different working fluids. In the same work, it was demonstrated that the optimum ambient temperature corresponding to the maximum exergy efficiency is 18.5 °C. Art and Arslan [16] proposed a system operating with a heat pump to supply the heating required for a city with a population of around 25000 and analyzed it thermodynamically and economically using 12 different working fluids in their case studies. Their simulation results indicated that if the number of residence increase, the net present value of the system would increase dramatically. Advanced exergoenvironmental analysis of geothermal district heating in the Afyon region was carried out by Yürüsoy and Keçebas [17]. Results revealed that the environmental degradation of the designed system is much lower compared to the traditional heating systems (wood-fired) and special attention should be paid to heat exchangers enhancement. Bursa geothermal district heating was analyzed thermodynamically by Yamankaradeniz [18] using advanced exergy principle. The main aim was to enhance the system performance via identifying the interactions among the components. Results of this study revealed that the conventional and advanced exergy efficiencies are around 0.25 and 0.26, respectively, and the priority of enhancement of system components was

heat exchangers followed by installed pumps. Researchers in [19] considered not only geothermal resource thermophysical condition, but also physical, and geochemical features of the wells in power plant selection in Turkey. A special attention was on the non-condensable gases existing in the geothermal resources which affect the type of power plant (binary, flash or combined binary-flash). Supplying the heating and cooling demand of the Aarhus University Hospital via solar assisted system was studied by Arabkoohsar and Andresen [20]. It was shown that during the summer the considered system could contribute around 30% to the heat preparation procedure of the chiller unit. Moreover, payback period of almost 2 years verified that the system is economically feasible in practice.

As observed from the reviewed literature and to the author's' best knowledge, there exists no standard configuration of a CCHP system to handle the most efficient use of geothermal sources. In addition, two main gaps were recognized in the literature. First, CCHPs have not been studied in depth for domestic purposes using a specified geothermal source for both summer and winter conditions. Second, most of the presented studies have addressed a specific operating point which makes it difficult to generalize the obtained results. The present study considers both mentioned gaps and gives a novel contribution to the field of geothermal energy usage for domestic applications via driving CCHPs. Therefore, in the present study, a domestic-scaled geothermal driven CCHP system is proposed and analyzed in detail using thermodynamic principles. B10 well in the Izmir-Balçova geothermal field [21] is considered as the source. Part of the geothermal fluid runs the ORC and produces space heating, while the rest drives an absorption chiller and then produces domestic hot water. The condenser of the ORC is also coupled with special heat exchangers to harvest the waste heat of ORC and contribute to space heating. Several working fluids are utilized in the ORC simulation and optimal operating points of the ORC and chiller are obtained. Exergoeconomic analysis is done to evaluate the economic feasibility of the system by calculating the payback period. In addition, exergy destruction within different components is obtained to measure efficiency along the process while a sustainability index is defined to evaluate the system from a sustainable development point of view. Finally, a sensitivity analysis is performed in detail to find the effects of the chiller supply and geothermal source condition on the system performance.

2. System description and assumptions

According to the previously mentioned facts about the importance of improving the share of utilizing geothermal sources in domestic applications in Turkey, this project proposes the employment of a specific geothermal well available in the Izmir-Balçova geothermal field (IBGF) to produce domestic heating, cooling, and electricity. Table 1 outlines some of the available details of the IBGF for the well numbered B-10. This well is selected as the case study in the simulation due to its appropriate temperature for domestic purposes.

Table 1

Main features of the considered geothermal well in Izmir-Balcova [21]

Well code	Set up year	Depth (m)	Temperature (K)	Volumetric flow rate (m^3/h)	Situation
B-10	1989	125	95-105	70-80	Production

A simplified schematic diagram of the proposed geothermal driven CCHP system is indicated in Fig. 1. The presented cogeneration system consists of a small-scale ORC, an absorption chiller providing desired cooling and heat exchangers to deliver hot water and required heat for space conditioning. Regarding the layout selection and components employment it should be noticed that the energy source temperature is the first determinative parameter. Simple ORC and single effect absorption chiller seem to be the most appropriate selection for this range of energy source. ORC is a completely developed and mature technology and has a wide application in the cases with low-medium temperature energy sources. Besides, compared to steam cycles, ORCs have enough flexibility, operate in lower pressure levels and have lower operating/maintenance costs [22–25]. In the presented system, geothermal fluid runs both ORC, via evaporation organic fluid within the ORC evaporator, and chiller via water vaporization within the generator. Under the base condition, half of the water is fed to run the ORC and the rest passes through the chiller. Evaporated organic fluid flows to the ORC turbine (ORCT) to turn the turbine blades and generate electricity via a coupled generator to the turbine shaft. Expanded organic working fluid enters the heat exchanger 1 (HE1) to heat the pressurized water, which delivers domestic space heating, and leaves it in a saturated liquid condition. In fact, HE1 performs as a wet condenser for the ORC harvesting waste heat of the ORC to use as domestic space heating. Finally, the employed pump (ORCP) increases the fluid pressure up to the ORCE pressure level and completes the ORC cycle. The ORCE exiting geothermal water is warm enough to provide domestic space heating so its heat content is transferred to the pressurized water to be utilized as domestic space heating. Another part of the geothermal fluid is used to run the chiller unit.

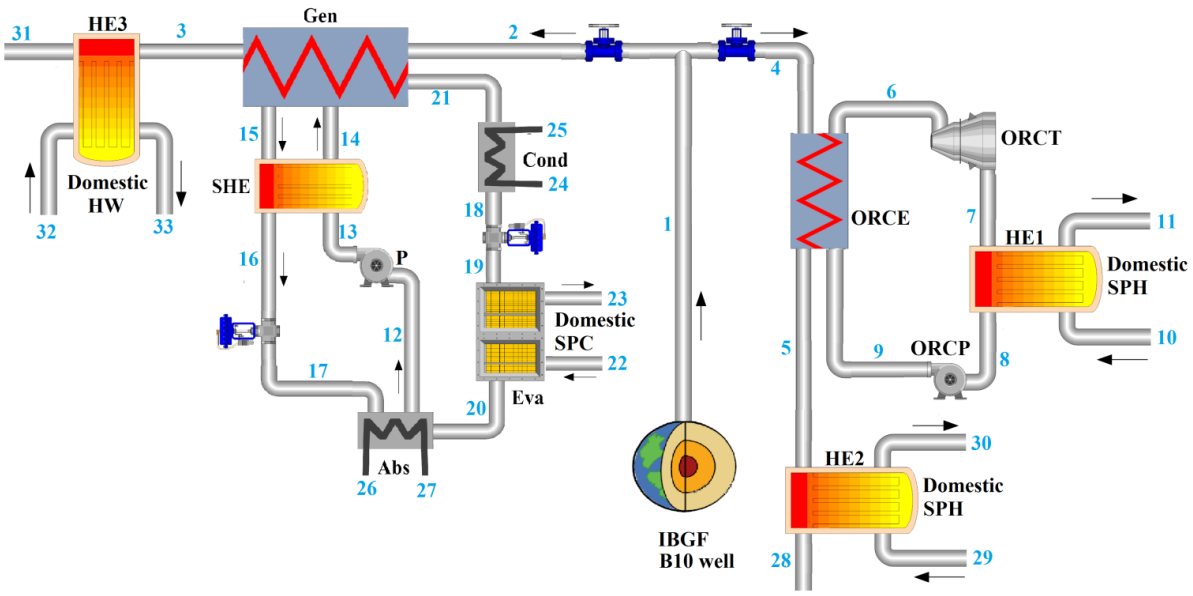

Fig. 1 Proposed geothermal driven CCHP system

Absorption chillers can be fueled by heat sources instead of electricity. Based on Dominković et al. [26] district cooling systems based on absorption chillers can bring significant socio-economic benefits in the hot and humid climate regions. Within the chiller unit, water and lithium bromide (LiBr) perform as refrigerant and absorbent, respectively. A solution of refrigerant (H_2O) and absorber (LiBr) exists within the absorber, while the absorber absorbs the refrigerant content. Afterthought, a pressure increasing process takes place for the combination of water and lithium bromide (strong solution). Then, this strong solution passes through the employed heat exchanger (SHE) and reaches the generator. Within the generator, the temperature of this solution increases and causes water content evaporation, which flows to the condenser. Meanwhile, the weak solution is fed back to the absorber while it absorbs the exiting refrigerant from the evaporator again. Lastly, Gen exiting geothermal fluid enters the HE3 to supply demotic hot water demand.

Regarding the presented system layout, it should be noticed that considering different climate conditions and changing system designing parameters may result in another layout (for instance, CHP instead of CCHP). Thereby, a change in the seasonal conditions (cold and warm days of the year) and a sensitivity analysis will be carried out in this study.

Steady state operating condition is supposed for the proposed cogeneration system [27]. It seems that this assumption makes the proposed system far from the real operating conditions. However, it should be noted that such geothermal-driven systems are developed to cover the base-load of the

grids. Then, considering this hypothesis seems to be logical. The main input data used in simulation studies and their values are listed in Table 2.

Table 2

Fixed value assumptions for the proposed geothermal-driven multi-generation system

Input data	Value	Unit
Geothermal volumetric flow rate [21]	70-80	m^3/h
Geothermal source temperature [21]	368-378	K
ORCT isentropic efficiency [28]	90	%
Pumps isentropic efficiency [29]	75	%
Efficiency of the electric generator [14]	95	%
Temperature of the coolant water	293	K
Temperature of pressurized water stream considered for DHW supply and return [30]	353 and 313	K
Temperature of pressurized water stream considered for SPH supply and return [31]	308 and 293	K
Temperature of pressurized water stream considered for SPC supply and return [20]	278 and 285	K
Generator temperature	348 - 358	K
Effectiveness of heat exchangers	85	%
Minimum temperature difference (pinch point) within ORCE, Eva and Cond	5	K
ORCE pressure	250 - 400	kPa

3. Thermodynamic model

Thermodynamic, thermos-economic, and sustainability assessment of the proposed CCHP is divided into different subsections to give the possibility of describing each section in detail. These subsections are presented hereunder.

3.1.Energy analysis

Thermodynamic analysis of the presented system is considered based on two main principles. Energy conservation and mass balance equations, as follows [32]:

$$\sum \dot{m}_i h_i + \dot{Q} = \sum \dot{m}_o h_o + \dot{W} \tag{1}$$

$$\sum \dot{m}_i = \sum \dot{m}_o \tag{2}$$

In fact, each component employed in the system is considered to be as an individual separate control volume. The energy conservation equations applied for the system components are listed hereunder in Table 3. It should be highlighted that equations 9, 11, 13, and 15 are derived from

definition of effectiveness for the employed heat exchangers and the corresponding value of the effectiveness is listed in Table 2.

Table 3
Energy conservation equation corresponding to the system main components [33–35]

Component	Equation	
ORCT	$\dot{W}_{ORCT} = \dot{m}_6 (h_6 - h_7)$	(3)
	$\eta_{is,ORCT} = \frac{\dot{W}_{ORCT}}{\dot{W}_{is,ORCT}}$	(4)
ORCE	$\dot{m}_4 (h_4 - h_5) = \dot{m}_9 (h_6 - h_9)$	(5)
ORCP	$\dot{W}_{ORCP} = \dot{m}_8 (h_9 - h_8)$	(6)
	$\eta_{is,ORCP} = \frac{\dot{W}_{is,ORCP}}{\dot{W}_{ORCP}}$	(7)
HE1	$\dot{m}_{10} (h_{11} - h_{10}) = \dot{m}_7 (h_7 - h_8)$	(8)
	$eff_{HE1} = \frac{Max\{(T_7 - T_8), (T_{11} - T_{10})\}}{T_7 - T_{10}}$	(9)
HE2	$\dot{m}_5 (h_5 - h_{28}) = \dot{m}_{29} (h_{30} - h_{29})$	(10)
	$eff_{HE2} = \frac{Max\{(T_5 - T_{28}), (T_{30} - T_{29})\}}{T_5 - T_{29}}$	(11)
HE3	$\dot{m}_3 (h_3 - h_{31}) = \dot{m}_{32} (h_{33} - h_{32})$	(12)
	$eff_{HE3} = \frac{Max\{(T_3 - T_{31}), (T_{33} - T_{32})\}}{T_3 - T_{32}}$	(13)
SHE	$\dot{m}_{15} (h_{15} - h_{16}) = \dot{m}_{13} (h_{14} - h_{13}),$	(14)
	$eff_{SHE} = \frac{Max\{(T_{15} - T_{16}), (T_{14} - T_{13})\}}{T_{15} - T_{13}}$	(15)
Gen	$\dot{m}_2 h_2 + \dot{m}_{14} h_{14} = \dot{m}_3 h_3 + \dot{m}_{15} h_{15} + \dot{m}_{21} h_{21}$	(16)
Cond	$\dot{m}_{21} (h_{21} - h_{18}) = \dot{m}_{24} (h_{25} - h_{24})$	(17)
Eva	$\dot{m}_{21} (h_{21} - h_{18}) = \dot{m}_{24} (h_{25} - h_{24})$	(18)
Abs	$\dot{m}_{20} (h_{20} - h_{19}) = \dot{m}_{22} (h_{22} - h_{23})$	(19)
P	$\dot{W}_P = \dot{m}_{12} (h_{13} - h_{12})$	(20)
	$\eta_{is,P} = \frac{\dot{W}_{is,P}}{\dot{W}_P}$	(21)

From the efficiency perspective, definition of energy utilization factor (EUF) is considered. The proposed system is supposed to supply the energy demands of a residential area in terms of electricity, space conditioning (in both hot and cold seasons), and domestic hot water. Then, a parameter which considers all these kinds of energy forms is necessary to evaluate the proposed

system from the first law of thermodynamic point of view. Then, EUF is an appropriate index for the systems with different products. For the examined system, this parameter can be defined as [36]:

$$EUF = \frac{\dot{W}_{net} + \dot{Q}_{SPH} + \dot{Q}_{DHW} + \dot{Q}_{SPC}}{\dot{m}_1 h_1} \tag{22}$$

in which, $\dot{W}_{net}$, $\dot{Q}_{SPH}$, $\dot{Q}_{DHW}$ and $\dot{Q}_{SPC}$ are the net supplied power, space heating, domestic hot water, and space cooling, respectively, to the domestic area. Mentioned parameters can be defined as follows [37,38]:

$$\dot{W}_{net} = \dot{W}_{ORCT} - \dot{W}_{ORCP} - \dot{W}_{P} \tag{23}$$

$$\dot{Q}_{SPH} = \dot{m}_{10}(h_{11} - h_{10}) + \dot{m}_{29}(h_{30} - h_{29}) \tag{24}$$

$$\dot{Q}_{DHW} = \dot{m}_{32}(h_{33} - h_{32}) \tag{25}$$

$$\dot{Q}_{SPC} = \dot{m}_{22}(h_{23} - h_{22}) \tag{26}$$

$\dot{W}_{ORCT}$, $\dot{W}_{ORCP}$ and $\dot{W}_{P}$ are determined in Table 3.

3.2.Exergy analysis

Exergy analysis can help to develop strategies and guidelines for more effective use of energy and has been applied to numerous thermal processes, including CCHPs. Exergy can be represented in terms of four components: physical, kinetic, potential, and chemical exergy [39]. Exergy is the maximum theoretic beneficial power (shaft work or electrical work) reachable as the systems interact to equilibrium, heat transfer occurring with the environment only [40]. A deep understanding of exergy definition can be found within the fundamental texts i.e., Kotas [41] or Szargut et al. [42]. Exergy balance equation for each component can be written as [43]:

$$\sum_j \dot{E}_{q,j} + \sum_i \dot{E}_i = \dot{W}_{cv} + \sum_e \dot{E}_e + \dot{E}_D \tag{27}$$

where $\dot{E}_i$ and $\dot{E}_e$ are exergy transfer rates at inlets and outlets, respectively, and $\dot{E}_q$, is the exergy rate associated with heat transfer. Non-usage exergies which are discharged to the environment (like the exergy rate associated with the condenser coolant before getting warm) are taken into account as the destroyed exergy. In the present study, kinetic, chemical (due to the absence of a change in the

composition), and potential exergies are ignored. Therefore, the only remaining term (physical exergy) and the rate of exergy in each state can be written as [44,45]:

$$e_{ph} = h - h_0 - T_0(s - s_0) \tag{28}$$

$$\dot{E} = m_i e_i \tag{29}$$

Providing the fuel-product definition ($\dot{E}_F$ and $\dot{E}_P$) in exergy analysis is convenient. Table 4 lists $\dot{E}_F$ and $\dot{E}_P$ for each system component. According to the provided information destroyed exergy and exergetic efficiency of each unit can be written as [46]:

$$\dot{E}_D = \dot{E}_F - \dot{E}_P \tag{30}$$

$$\varepsilon = \frac{\dot{E}_P}{\dot{E}_F} \tag{31}$$

Table 4

Developed exergy balance equations for the designed multi-generations system components [47–49]

Component	$\dot{E}_F$	$\dot{E}_P$	**Destroyed exergy**	
ORCT	$\dot{E}_6 - \dot{E}_7$	$\dot{W}_{ORCT}$	$\dot{E}_6 - \dot{E}_7 - \dot{W}_{ORCT}$	(32)
ORCE	$\dot{E}_4 - \dot{E}_5$	$\dot{E}_6 - \dot{E}_9$	$\dot{E}_4 + \dot{E}_9 - (\dot{E}_5 + \dot{E}_6)$	(33)
ORCP	$\dot{W}_{ORCP}$	$\dot{E}_9 - \dot{E}_8$	$\dot{W}_{ORCP} + \dot{E}_8 - \dot{E}_9$	(34)
HE1	$\dot{E}_7 - \dot{E}_8$	$\dot{E}_{11} - \dot{E}_{10}$	$\dot{E}_7 + \dot{E}_{10} - (\dot{E}_8 + \dot{E}_{11})$	(35)
HE2	$\dot{E}_5 - \dot{E}_{28}$	$\dot{E}_{30} - \dot{E}_{29}$	$\dot{E}_5 + \dot{E}_{29} - (\dot{E}_{28} + \dot{E}_{30})$	(36)
HE3	$\dot{E}_3 - \dot{E}_{31}$	$\dot{E}_{33} - \dot{E}_{32}$	$\dot{E}_3 + \dot{E}_{32} - (\dot{E}_{31} + \dot{E}_{33})$	(37)
SHE	$\dot{E}_{15} - \dot{E}_{16}$	$\dot{E}_{14} - \dot{E}_{13}$	$\dot{E}_{15} + \dot{E}_{13} - (\dot{E}_{14} + \dot{E}_{16})$	(38)
Gen	$\dot{E}_2 - \dot{E}_3$	$\dot{E}_{21} + \dot{E}_{15} - \dot{E}_{14}$	$\dot{E}_2 + \dot{E}_{14} - (\dot{E}_3 + \dot{E}_{21} + \dot{E}_{15})$	(39)
Cond	$\dot{E}_{21}$	$\dot{E}_{18}$	$\dot{E}_{21} - \dot{E}_{18}$	(40)
Eva	$\dot{E}_{20} - \dot{E}_{19}$	$\dot{E}_{23} - \dot{E}_{22}$	$\dot{E}_{20} + \dot{E}_{22} - (\dot{E}_{19} + \dot{E}_{23})$	(41)
Abs	$\dot{E}_{20} + \dot{E}_{17}$	$\dot{E}_{12}$	$\dot{E}_{20} + \dot{E}_{17} - \dot{E}_{12}$	(42)
P	$\dot{W}_P$	$\dot{E}_{13} - \dot{E}_{12}$	$\dot{W}_P + \dot{E}_{12} - \dot{E}_{13}$	(43)

3.2.1. *Exergy efficiency*

An exergetic efficiency for the proposed residential-scaled CCHP can be calculated as the percentage of the exergy supplied to the system that is recovered in the product of the system. Then, total exergetic efficiency of the proposed system can be written as [50,51]:

$$\varepsilon = \frac{\dot{W}_{net} + \dot{E}_{11} - \dot{E}_{10} + \dot{E}_{30} - \dot{E}_{29} + \dot{E}_{33} - \dot{E}_{32}}{\dot{E}_1} \tag{44}$$

3.2.2. *Sustainability assessment*

Before conducting the sustainability analysis, it should be highlighted that sustainable development has been defined in different ways, but the most frequently used definition refers to "a development that meets the needs of the present without compromising the ability of future generations to meet their own needs" [52]. In fact, sustainability assessment is an index of sustainable development [53] which emphasizes the efficient use of energy sources with the lowest energy loss values. In this regard, sustainability and exergy analysis are highly correlated to each other which in turn help to define the sustainability index as follows [54,55]:

$$SI = \frac{1}{D_P} \tag{45}$$

where,

$$D_P = \frac{\dot{E}_D}{\dot{E}_{in}} \tag{46}$$

In the equation above, $\dot{E}_{in}$ is the rate of total input exergy to the system.

3.3.*Exergoeconomic analysis*

Exergoeconomics principle combines the role of exergy analysis and conventional economic evaluation to estimate the cost effectiveness of the energy systems. This method provides economical information not obtainable by exergy or economic analysis separately. The main aim of this exergy based economic analysis is to determine the unit cost of products. Hereunder, the SPECO (specific exergy costing) method is adopted for the proposed geothermal-driven cogeneration system. Exergy analysis and obtaining the rate of exergy for each point of the system is required for exergoeconomic analysis, which has been described in previous sections in detail. Thereby, adopting balance equations for each component is the next step.

3.3.1. Cost balance

Developing the cost balance relationships for each system component is required for exergoeconomic assessment, which can be written as:

$$\sum_{e} \dot{C}_{e,k} + \dot{C}_{w,k} = \dot{C}_{q,k} + \sum_{i} \dot{C}_{i,k} + \dot{Z}_k \tag{47}$$

$$\dot{C}_j = c_j \dot{E}_j \tag{48}$$

In the equations above, $\dot{C}$ is the cost rate of each stream in terms of \$/s, $\dot{Z}_k$ is the time-dependent capital cost rate of the kth component and can be obtained as:

$$\dot{Z}_k = Z_k . CRF . \varphi / (3600N) \tag{49}$$

$$CRF = \frac{i(1+i)^m}{(1+i)^m - 1} \tag{50}$$

where, m is the system life and i is the interest rate. φ is the maintenance factor (1.06), CRF is the capital recovery factor, and N is the number of system operating hours in a year [56]. Table 5 outlines the cost functions associated with these components.

Table 5 Cost functions of the main components employed in the proposed system [57]

Component	Cost function	
Gen	$Z_{Gen} = 17500 \, (\frac{A_{Gen}}{100})^{0.6}$	(51)
Eva	$Z_{Eva} = 16000 \, (\frac{A_{Eva}}{100})^{0.6}$	(52)
Abs	$Z_{Abs} = 16000 \, (\frac{A_{Abs}}{100})^{0.6}$	(53)
Cond	$Z_{Cond} = 8000 \, (\frac{A_{Cond}}{100})^{0.6}$	(54)
P	$Z_{ORCP} = 2100 (\frac{\dot{W}_{ORCP}}{10})^{0.26} (\frac{1-\eta_{ORCP}}{\eta_{ORCP}})^{0.5}$	(55)
ORCT	$Z_{ORCT} = 4750 \dot{W}_{ORCT}^{0.75}$	(56)
ORCP	$Z_{ORCP} = 200 \dot{W}_{ORCP}^{0.65}$	(57)
ORCE	$Z_{ORCE} = 309.14 A_{ORCE}^{0.85}$	(58)
HE1	$Z_{HE1} = 309.14 A_{HE1}^{0.85}$	(59)
HE2	$Z_{HE2} = 309.14 A_{HE2}^{0.85}$	(60)
HE3	$Z_{HE3} = 309.14 A_{HE3}^{0.85}$	(61)
SHE	$Z_{Cond} = 8000 \, (\frac{A_{Cond}}{100})^{0.6}$	(62)

To evaluate the economic performance of the proposed residential-scaled CCHP, the net present value (NPV) method [36] is utilized as follows:

$$NP_0 = \sum_{z=0}^{BL} Y_z (1+i)^{-z} \tag{63}$$

here, Y_z is the net cash flow at the end of the z^{th} period, BL refers to the system economic life and i is the interest rate. It is supposed that the income cash flow is achievable at the end of each year, interest rate and BL are 4% and 20 years, respectively [57]. Annual incomes associated with the systems referred to the produced power and heat are also supposed to be 30 and 20 €/MWh, respectively [58,59].

4. Results and discussion

To obtain the energy and exergy values accessible in the geothermal resource and corresponding to different source temperature, thermophysical properties of material available within the EES software [60] are utilized. A specified mass flow rate of 75 m^3/h is also considered for the candidate source. Hereby, the accessible energy and exergy content of the source refers to the difference between energy and exergy of the geothermal source associated with the source and ambient temperatures. Table 6 is listed energy and exergy content of the geothermal water for different resource temperatures.

Table 6

Energy and exergy content of the candidate geothermal resource

Geothermal resource temperature (°K)	**368**	**373**	**378**
Available thermal energy (kW)	6107	6546	6986
Available thermomechanical exergy (kW)	621.6	707.8	798.8

To validate the obtained results, the data reported in the literature is used [61]. Since a simple ORC is employed in the proposed CCHP, the validation is performed for the simple ORC as studied in [61], comprehensively. In [61], a simple ORC is utilized to produce electricity from a specified geothermal resource. Exergy destruction within the ORC components is compared under the same conditions, while databases utilized for the working fluid's thermophysical properties in both studies are the listed data in the library of the EES. Table 7 outlines this comparison. Referring to this table, a good agreement exists between the results obtained in this study and those reported by the literature [61].

Table 7

Comparison of the results with those of reported in the literature for the case of simple ORC.

Component	Exergy destruction reported by the Shokati et al. (kW)	Obtained exergy destruction (kW)
Evaporator	625.5	623
Turbine	762.1	764
Preheater	1099.0	1088
Pump	21.2	18
Condenser	278.7	278

To evaluate the performance of the employed ORC and absorption chiller two key parameters exist, namely ORCE pressure level and Gen temperature. Since the thermodynamic implementation of the ORC and absorption chiller affects the whole system performance, optimum values of ORCE pressure and Gen temperature are obtained. Referring to Fig. 2, generator operating temperature of 353 K leads to a maximum coefficient of performance (COP) for the chiller unit. Thereby, this value is supposed to be the generator temperature for the rest of the simulation.

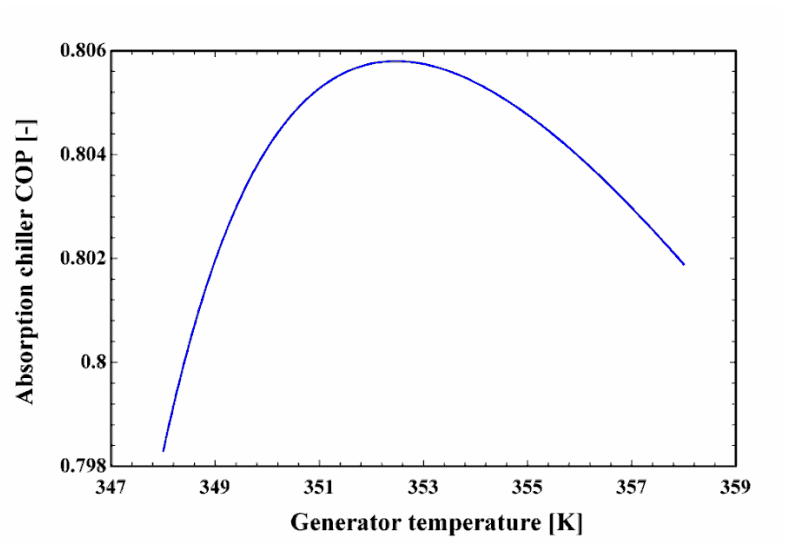

Fig. 2 Different COP values corresponding to the various generator temperature

The employed evaporator in the ORC (ORCE) is the component in which the evaporation process of organic fluid occurs due to heat transfer from geothermal water. Fig. 3 illustrates this process within the evaporator, which is known as the T-Q diagram. Several organic compounds are considered as the working fluid in the ORC simulation and the effect of the change in the ORCE pressure level is investigated. According to Fig. 4, the net produced power by the ORC takes a

maximum value in special value of evaporator pressure. To explain this, it should be stated that a change in the ORCE pressure level increases the turbine inlet pressure, while decreases the evaporated fluid mass flow rate. The former increases the outlet power, while the latter decreases it. Then maximizing net produced power by the ORC higher pressure is justified. Referring to Fig. 4, utilizing different working fluids has no considerable effect on the maximum output power. This is while the optimum pressure corresponding to the maximum power for the case of R123 is much lower than those of other cases. Thereby, R123 is chosen as the working fluid in the rest of the results. The same results have been shown by Alrahimi et al. [62], comparing the performance of R123 with nine different refrigerants. Table 8 outlines the properties of R123 as the selected working fluid.

It should be noted that the use of R123 will be banned by the Montreal protocol. However, this usage-ban has not been applied yet. For the time being, not only this refrigerant is used in a wide spectrum of research and practical works, but also it is well-proved that this refrigerant performs better than other commercially available refrigerants [62,63].

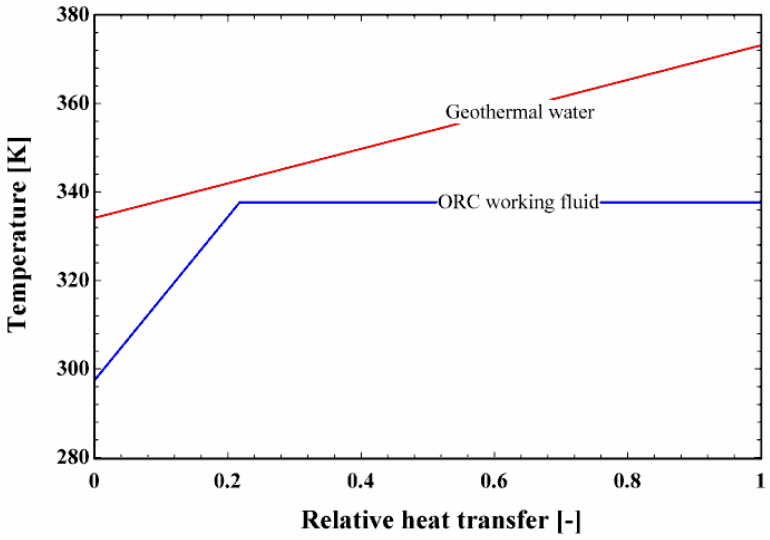

Fig. 3 T-Q diagram corresponding to the employed ORCE

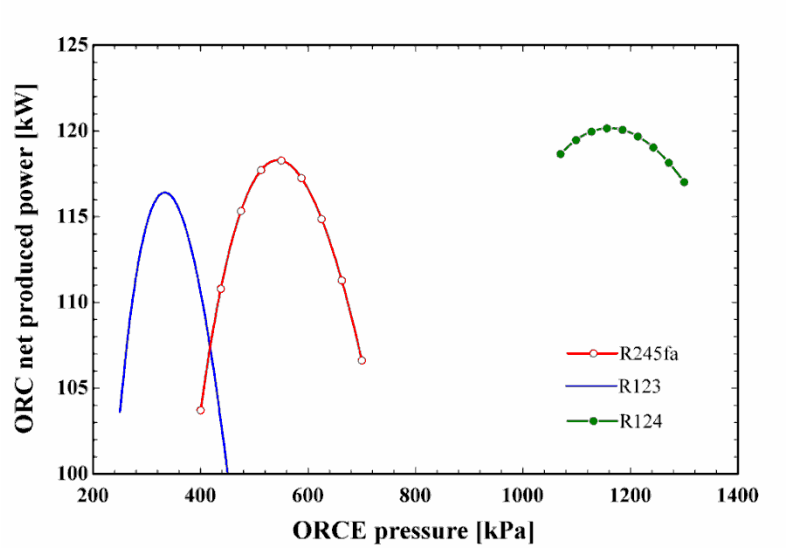

Fig. 4 ORC pressure level versus the ORC net produced power using different working fluids

Table 8

Thermophysical properties of the R123 as the selected organic working fluid [60,64].

Compound	Molecular weight (kg/kmol)	Critical temperature (˚C)	Critical pressure (bar)	Boiling temperature at 1 atm (°C)	Eccentric Factor
R123	152.9	183.7	36.7	27.8	0.2821

Table 9 represents the results and technical parameters extracted from the system simulation. In this section, it is supposed that 50% of the geothermal resource is utilized to run the ORC and half of the water is supplied to drive the absorption chiller and produce domestic hot water. However, simulations are done for different values of chiller supply rate (mass flow rate ratio between streams 1 and 2) and results will be presented in the following. Temperature and volumetric flow rate of 373 K and 75 m^3/h, respectively, is considered for the geothermal source. Also, ORC and absorption chiller perform under the optimized condition from the net produced power and COP points of view, respectively. Referring to the same table, the proposed system generates 116.3 kW electricity with ORC thermal efficiency of 6.8 %. It should also be highlighted that the delivered SPH via heat exchanger 1 is completely considerable (1590 kW). This value of heating is recovered from non-usage energy of the ORC condenser. EUF as the overall thermal efficiency of the proposed multi-generation system is obtained to be 55.9 %. Also, overall exergy efficiency and payback period of 49.6% and 4.6 years are obtained, respectively. Other parameters like mass flow rate of heat carrying fluids are also reported in table 9, which are determinative parameters for heat exchanger designers.

Table 9

Results of the system simulation

Input data	Value	Unit
Net produced power	116.3	kW
SPH via HE1	1590	kW
SPH via HE2	1428	kW
SPC via evaporator	529.7	kW
DHW via HE3	1744	kW
Mass flow rate of ORC working fluid	8.7	Kg/s
Mass flow rate of pressurized water in HE1	25.3	Kg/s
Mass flow rate of pressurized water in HE2	22.8	Kg/s
Mass flow rate of pressurized water in HE3	10.4	Kg/s
Mass flow rate of cold water in Eva	25.3	Kg/s
ORC efficiency	6.8	%
Absorption chiller COP	0.8	-
EUF	55.9	%
Exergy efficiency	49.6	%
Payback period	4.6	year

As stated before, unlike the energy analysis, exergy evaluation addresses the exact location and values of irreversibilities within the system. In fact, exergy is not conserved and exergy destruction happens in each real thermodynamic process because of both internal and external inefficiencies. Hereunder special focus has paid on the destroyed exergy within each main component employed in the system. In addition, the exergetic performance of the components is evaluated and second law efficiency is carried out.

The breakdown of exergy destruction within the entire system is shown in Fig. 5. The main exergy destructive unit is the generator implemented in the absorption chiller mainly due to the water content evaporation within this unit and causes 24% of total destroyed exergy. Following the same analysis, the employed evaporator in the ORC is the second exergy destructive component and 21% of total destroyed exergy is due to irreversibilities within this component. Apparently, destroyed exergy in this component happens due to the temperature mismatch between hot and cold streams (see Fig. 3). The third important component that is involved in the exergy destruction is heat exchanger 2 with 19% of total exergy destruction. Exergy destruction results reveal that these three components are the sources of almost 64% of total exergy destruction. Therefore, to enhance the

exergetic performance of the entire system, any improvement for the mentioned components is highly recommended.

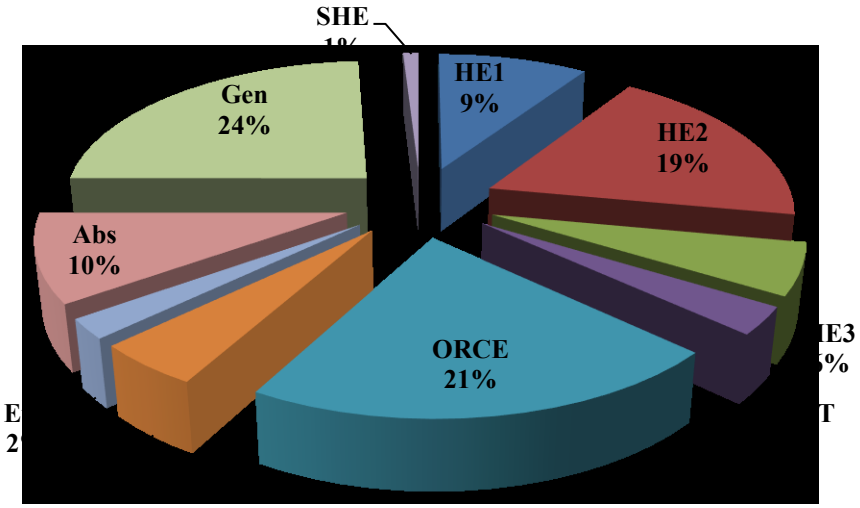

Fig. 5 Share of each component in total exergy destruction

The exergy efficiency of the system components is presented in Fig 6. Components with the lower second law efficiency are always matters of concern meaning that any improvement in their exergetic performance could increase the system exergy efficiency. As can be seen, the lowest exergy efficiency belongs to the heat exchanger 2 followed by heat exchanger 1. It is worth mentioning that both heat exchangers 1 and 2 have a lower exergy efficiency compared to the heat exchanger 3. This is because entering geothermal fluid to these heat exchangers is relatively low temperature and has low exergy. Therefore, transferring low quality energy to pressurized water stream in these heat exchangers leads to lower exergy efficiency. *T*-*Q* diagrams of heat exchangers are illustrated in Fig. 7. Here, *Q* is defined as the ratio of the transferred heat at each position to the total transferred heat in the heat exchanging device. Better temperature matching of the streams in a heat exchanging device leads to lower exergy destruction. This is clear since temperature difference is one of the main irreversibility sources. In the diagrams presented in this figure, temperature mismatching between cold and hot streams reveals the irreversibility within the heat exchanger and more difference between hot and cold streams temperature glide results in more exergy destruction. Furthermore, as it was expected, the highest exergy efficiency among the all refers to the ORCT and this is mainly due to avoiding droplet erosion within the ORCs expander and allowing for reliable operation, as reported in the literature [65].

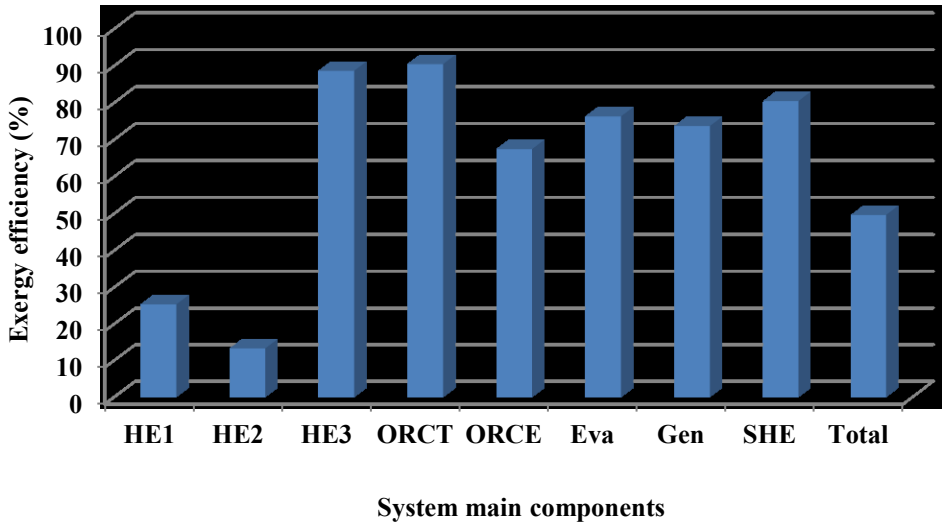

Fig. 6 Exergy efficiency of the system components

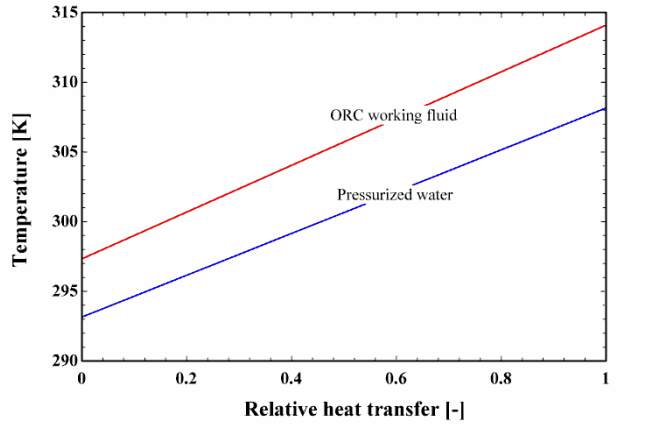

(a)

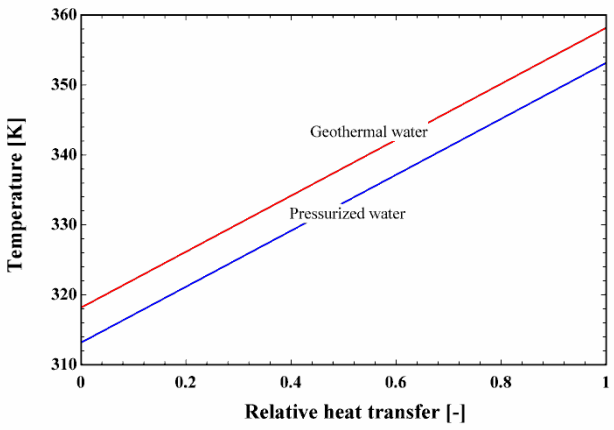

(b)

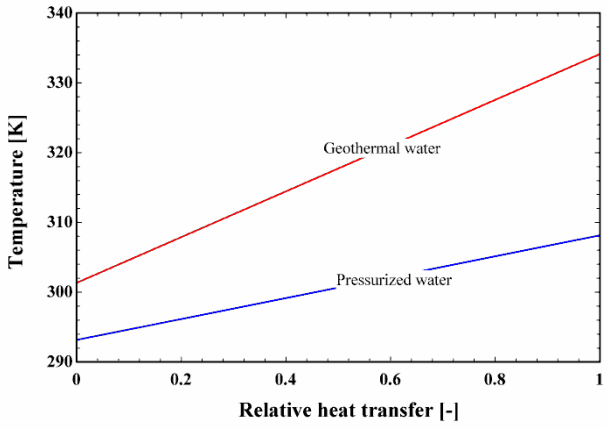

(c)

Fig. 7 T-Q diagram of a) HE1, b) HE2, c) HE3

The overall exergy efficiency of 49.6 indicates that almost half of geothermal exergy is converted to electricity, space heating, space cooling, and hot water demand. Obtained exergy efficiency is completely comparable with those reported in the literature [66,67] for the geothermal driven CCHPs. Besides, the sustainability index of around 2.0 is obtained for the proposed system, which is higher than the relevant geothermal based energy systems [68] and specifies the importance of the proposed system environmentally. In fact, the sustainability index is considered as the relation between thermodynamics performance and environmental impact in the present study.

4.1.Sensitivity analysis

Having the results associated with thermodynamic analysis corresponding to specific values of the chiller (or ORC) supply and geothermal source condition, one could understand the importance of a change in these parameters on the overall system performance. Four parameters are defined to obtain the results for different operating cases, which allows results to be generalized instead of being valid for a specific operating condition. These parameters are as follows:

- Ambient temperature
- Chiller supply mass flow rate ($\frac{m_2}{m_1}$)
- Geothermal source volumetric flow rate
- Geothermal source temperature

Fig. 8 illustrates exergy efficiency of the proposed geothermal-driven CCHP plant under the base condition. As was expected, during summertime, the exergy efficiency of the system decreases mainly due to a reduction in the exergy rate associated with the supplied district heating. In fact, during the cold days, as the ambient temperature decreases, the temperature difference between dead state (which is important from the exergy point of view) and delivered district heating increases. During the entire year, exergy efficiency of the system varies between 40.6 and 53.46 %.

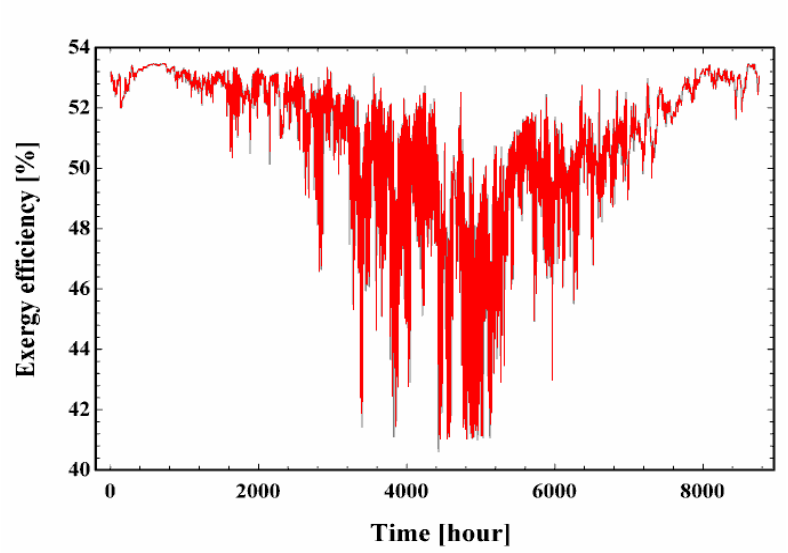

Fig. 8 Exergetic efficiency of the proposed system ambient temperature over the entire year

Fig. 9, presents the variation in the thermodynamic performance and sustainability of the proposed system, while geothermal temperature and volumetric flow rate of 373 K and 75 m^3/h are considered, respectively. Referring to this figure, increasing chiller supply continuously decreases the energy utilization factor of the system as the first law efficiency. Changing chiller supply from 0.01 to 0.99 reduces the energy utilization factor from 71.5 to 41.3%. The energy utilization factor of the system depends on the net produced power by the ORC, rate of space heating/cooling, and rate of supplied domestic hot water. In fact, increasing $\frac{m_2}{m_1}$ decreases net produced power by the ORC and heating associated with domestic heating, while increases delivered cooling and supplied domestic hot water. These parameters are shown in Fig. 10. This figure depicts the trends of such parameters affecting the thermodynamic performance of the proposed CCHP. Since the EUF parameter is a function of domestic space heating/cooling, domestic hot water, and net produced power by the ORC, these parameters are illustrated in Fig. 10. Based on Fig. 10, reduction in space heating is relatively intensive and has more effect on the EUF behavior. As mentioned before, heat delivery for space heating demand occurs in two stages, harvesting waste energy from the ORC condenser and energy recovery from the geothermal reinjection. Thus, decreasing the mass flow rate of geothermal water which runs the ORC has a significant effect on the delivered space heating.

Furthermore, increasing chiller supply leads to an improvement in the exergetic performance and sustainability of the system. Referring to Fig. 9, it is observed that exergy efficiency in such energy systems is linked with system sustainability which clarifies the relation between second law analysis and environmental impact. System total exergy efficiency depends on the exergy rates

associated with space heating/cooling, supplied domestic hot water, and rate of outlet power by the ORC. These parameters are shown in Fig. 11 and vary in such a way that results in increasing the system exergy efficiency. When $\frac{m_2}{m_1}$ varies from 0.01 to 0.99 the exergy efficiency grows from 40.0 to 59.3%. The most determinative parameter in the exergy efficiency trend is the exergy rate in conjunction with domestic hot water and increases from 3.6 to 359.2 kW, as Fig. 11 depicts. So, the behavior of the exergy efficiency with $\frac{m_2}{m_1}$ can be justified.

Based on the obtained results, it seems that higher values of chiller supply are favorable from the exergy perspective. But, parallel to the exergy efficiency of CCHPs, electricity generation can be of interest. This is because, first, electricity is strongly more valued compared to heating/cooling in the European energy market. Second, European heat sectors are based on efficient electricity-driven instruments, e.g. heat pumps, as reported by Nami and Arabkoohsar [30].

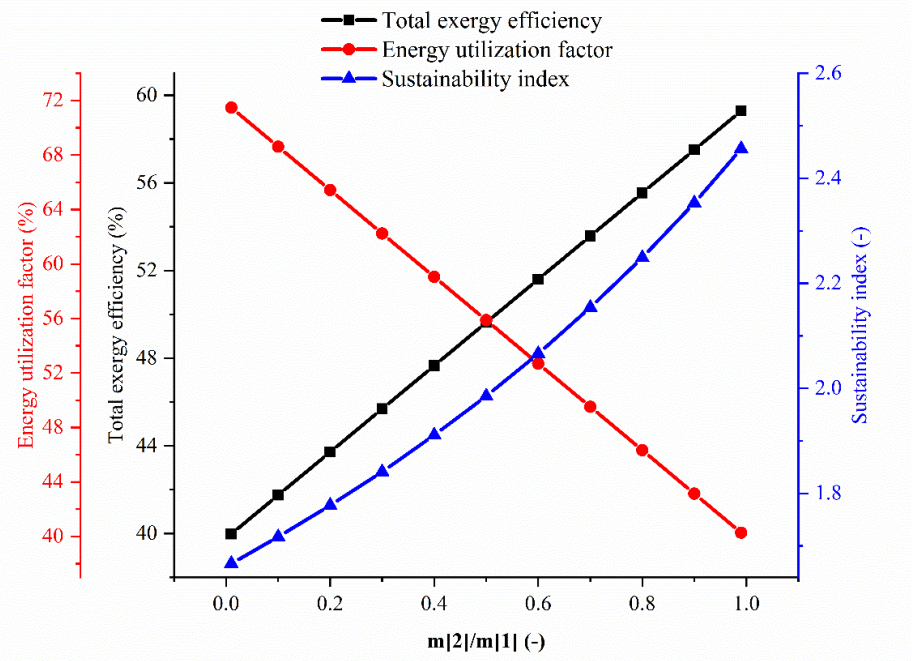

Fig. 9 Change in the system performance with chiller supply ($\frac{m_2}{m_1}$)

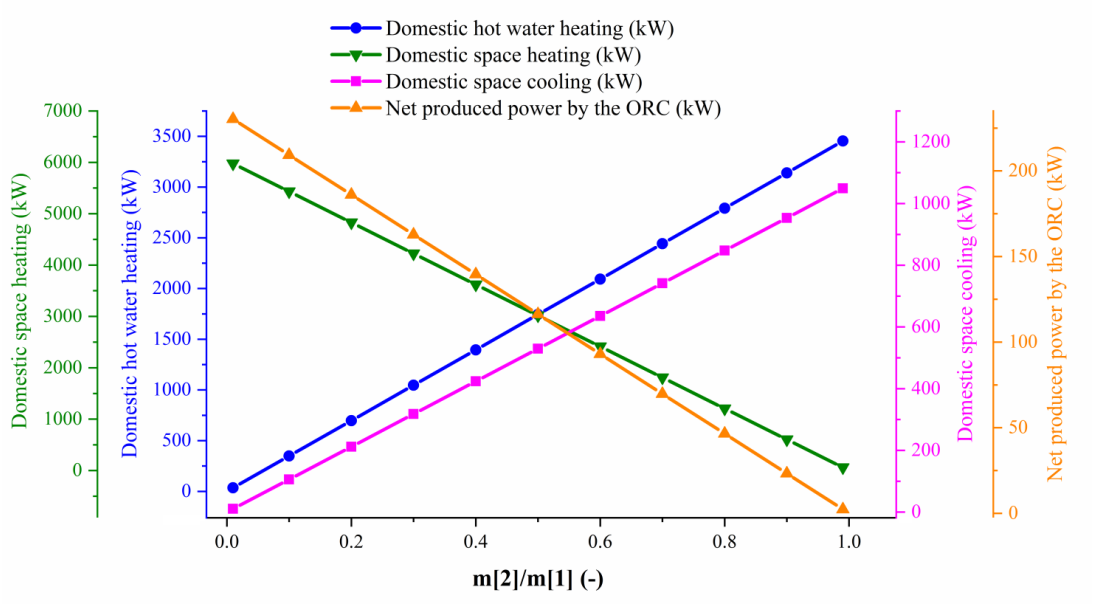

Fig. 10 Effect of chiller supply ($\frac{m_2}{m_1}$) on the system thermodynamic parameters

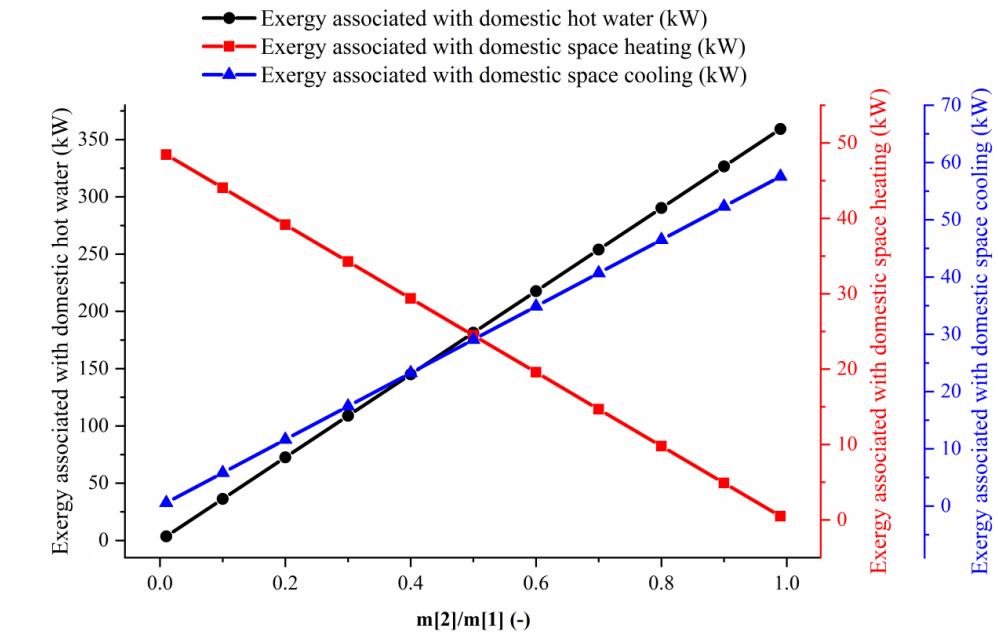

Fig. 11 Effect of chiller supply ($\frac{m_2}{m_1}$) on the system exergetic parameters

To evaluate the effects of the geothermal source thermophysical condition on the proposed system operation, optimal ORCE pressure should be obtained corresponding to each source temperature. Table 10 lists the optimal ORCE pressure for each source temperature corresponding to the maximum ORC output power. It should be noted that the geothermal resource volumetric flow rate

does not affect the optimized pressure of the ORC. The obtained pressure levels outlined in Table 10 are utilized in the source condition sensitivity analysis. Also, it is worth noting that the range of considered geothermal source temperature and the volumetric flow rate is taken out from real data for the Izmir-Balçova geothermal region.

Table 10

Optimal ORCE pressure corresponding to the maximum ORC output power for different geothermal sources temperatures

Source temperature (K)	**368**	**369**	**370**	**371**	**372**	**373**	**374**	**375**	**376**	**377**	**377**
Optimal pressure (kPa)	311.2	314.3	318.8	323.5	328	334.2	338.8	343.3	348	354.1	358.5

The effects of the geothermal source condition on the proposed system performance are shown in Figs. 12-14, when half of the geothermal water is supplied to run the chiller. As can be seen from these figures, change in the geothermal flow rate has no considerable effect on system performance. In fact, a change in the geothermal flow rate varies all the products of the system (electricity, heating, and cooling) and input energy to the system as well. These changes take place in such a way that the ratio of products to the input energy (as a definition of energy utilization factor) remains constant. As the figures show, unlike the geothermal flow rate, source temperature has a remarkable effect on system performance. Referring to these figures, increasing source temperature weakens the system thermodynamic performance and sustainability. When the source temperature rises from 368 to 378 K the EUF, ε and SI parameters reduce from 56.22%, 51.74, and 2.07 to 55.38%, 48.01, and 1.93, respectively. This is while the products of the proposed geothermal-driven CCHP system in terms of energy and exergy should be increased in cases of operating with warmer geothermal fluid. The key point is increasing the available energy and exergy in the geothermal source by increasing its temperature. In fact, the slope of the variation in the available energy and exergy in the geothermal source with a change in the source temperature is more intensive than those related to the system products (see Fig. 15). In other words, the effect of increasing the rate of input energy/exergy to the system is more the effect of increasing the rate of energy/exergy associated with the system products. Therefore, decreasing the energy and exergy performance of the system with increasing source temperature can be justified.

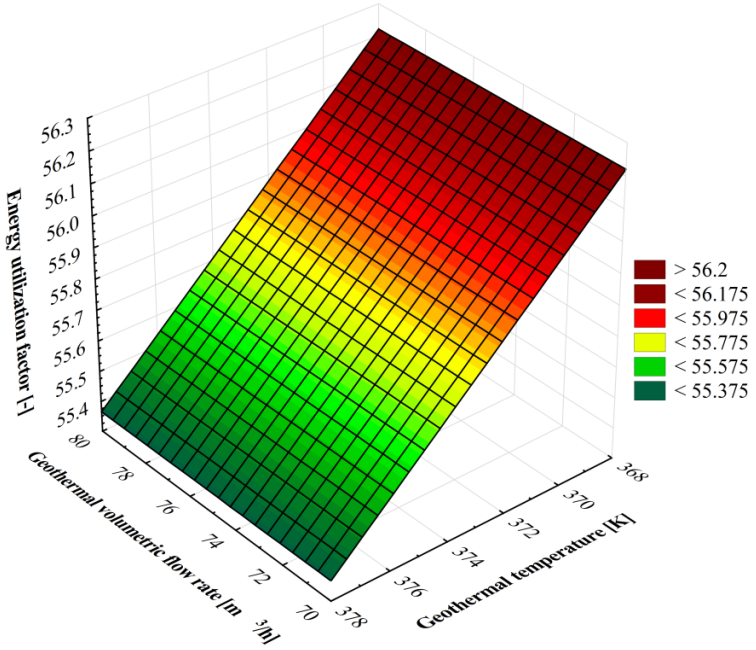

Fig. 12 Energy utilization factor versus geothermal source condition

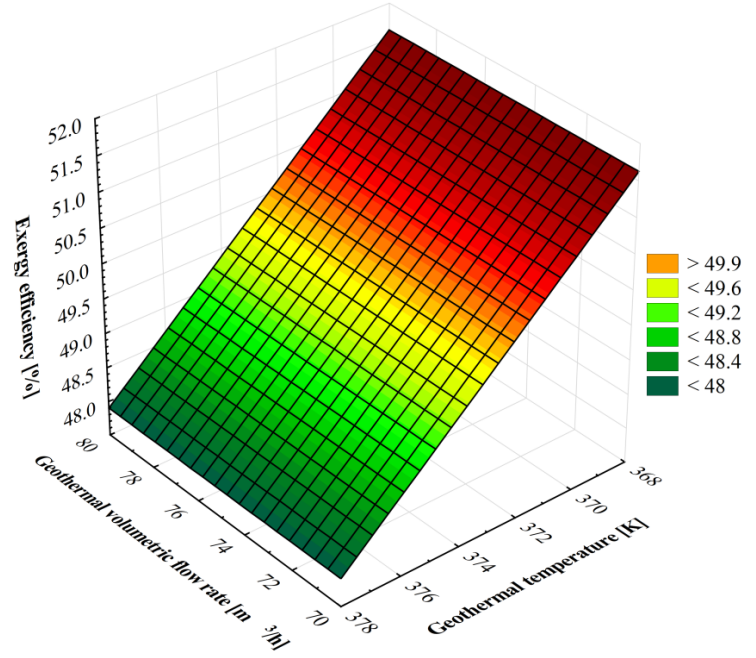

Fig. 13 Exergy efficiency versus geothermal source condition

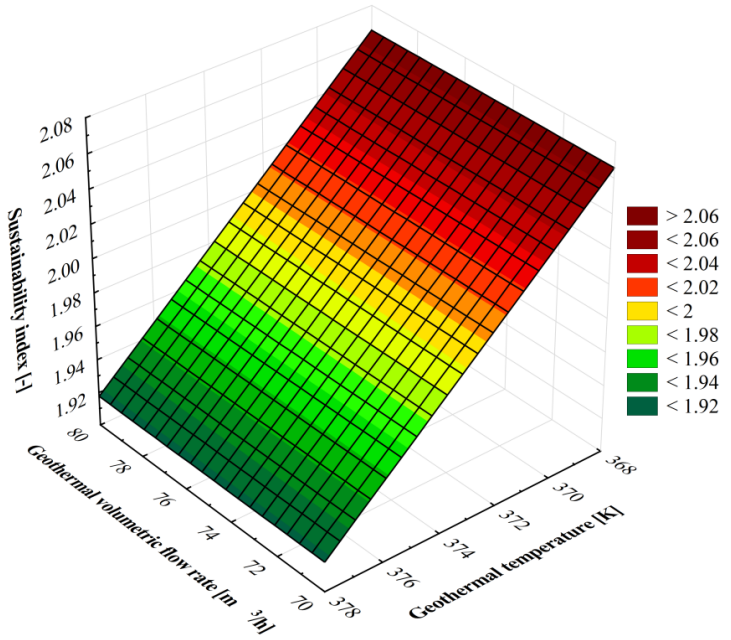

Fig. 14 Sustainability index versus geothermal source condition

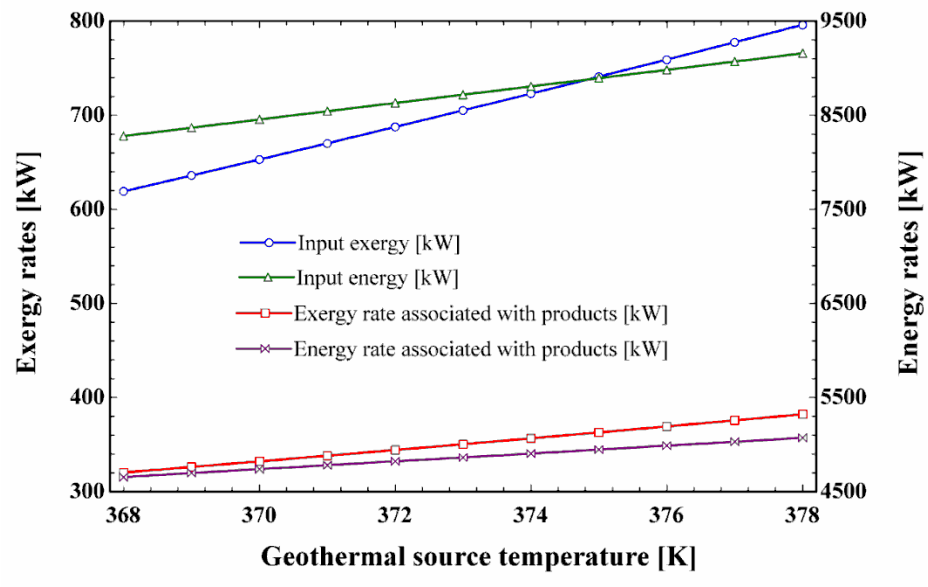

Fig. 15 Geothermal resource temperature versus the rate of input energy/exergy and the rate of energy/exergy associated with the system products

4.2.Operating under different seasonal conditions

That the cooling and heating demand may vary during different seasons is an admissible fact. Besides, the proposed system is designed in such a way that any change in the cooling demand will automatically affect the heating demand and it allows the system to be operated with acceptable

flexibility. Consequently, it is decided to evaluate the performance of the proposed CCHP plant for both summertime and wintertime conditions. Besides, the base technical assumptions (listed in Table 1) are considered to be the same for both cases with geothermal temperature and volumetric flow rate of 373 K and 75 m3/h, respectively. Also, it is considered that during the cold days space heating demand reaches its maximum amount, while there is no space heating demand for hot days of the year. Then, during the summertime, harvested heat from the HE1 (condenser of the ORC) will be wasted without any usage and HE2 will not be operated. Moreover, it is assumed that during the hot days of the year there is still a requirement for domestic hot water. This is while, for the cold days of the winter, geothermal water does not pass the chiller (i.e., required space cooling is assumed zero), and the proposed CCHP system turns into a CHP plant (see Fig. 16). Under this condition, a variable demand for domestic hot water is considered. The maximum value of hot water production means zero power and space heating production, while minimum hot water production reflects the maximum power production and space heating as well. The results of the simulation for both hot and cold days are listed in Table 11.

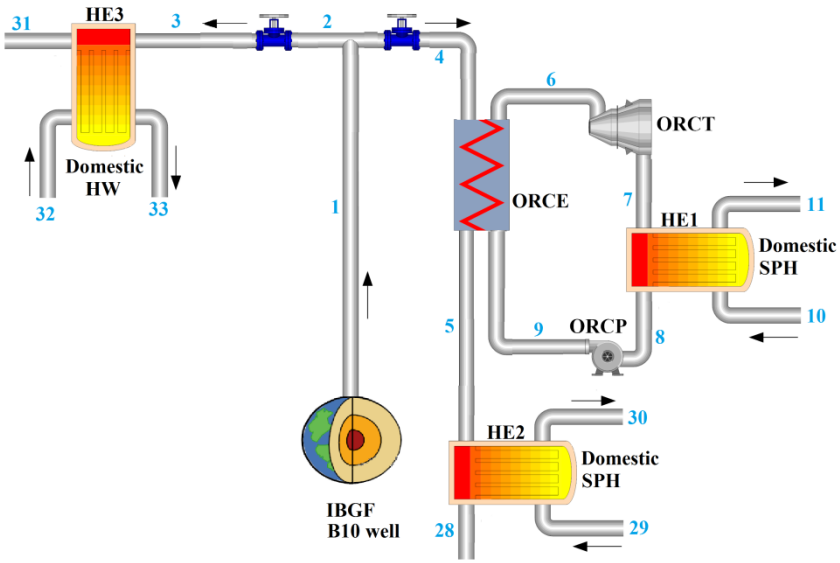

Fig. 16 Configuration of the CHP plant operating in the wintertime condition

As can be observed, to reach higher values of the first and second law efficiencies in the summertime, higher cooling and domestic hot water production are recommended. Fortunately, during the hot days of the year cooling demand increases and as stated before, there is still a requirement for hot water. Higher values of energy and exergy contents associated with domestic hot water are the main reason for this operating condition.

During the cold days, supplied heating for space conditioning (with a considerable value of energy and exergy) comes into account in the thermal and exergetic performance of the designed system. Therefore, the performance of the system improves in this condition, compared to summertime. According to Table 9, during the summer season, when the supplied cooling for space conditioning comes down from 1058 to 0 kW (from maximum power production to the minimum) the EUF decreases from 52.04 to 2.67%, exergy efficiency reduces from 59.45 to 32.87% and sustainability index declines from 2.466 to 1.49. Also, during the wintertime, when the domestic hot water demand changes from 4612 to 0 kW the EUF increases from 53.54 to 71.78%, exergy efficiency reduces from 68.17 to 39.81% and sustainability index declines from 3.14 to 1.66.

Table 11

Technical parameters of the proposed multi-generation energy system under different seasonal conditions

Parameter (unit)	Summer season	Winter season
Net produced power (kW)	0-232.6	0-232.6
Delivered SPH (kW)	0	0-6029
Delivered SPC (kW)	1058-0	0
Delivered DHW (kW)	3485-0	4612-0
EUF (%)	52.04-2.67	53.54-71.78
Total exergetic efficiency (%)	59.45-32.87	68.17-39.81
SI (-)	2.47-1.49	3.14-1.66

5. Conclusion

In this study, a geothermal driven CCHP was proposed and analyzed in detail using thermodynamic and sustainability principles. The system was designed to supply power (as electricity consumption), heating (for both space heating and domestic hot water) and cooling (for space cooling). A set of real data was utilized as the geothermal source condition and B10 well in the Izmir-Balçova region was considered as the source candidate. The idea was developed mainly since developing renewable-based, especially geothermal-driven, energy systems are attracting more attention day by day in developing countries like Turkey. To this end, a configuration for the electricity, heating and cooling production was proposed and a detailed energy and exergy analysis was accomplished. In addition, a parametric study was carried out to show the effect of any change

in the decision parameters on the system performance. Furthermore, the designed multi-generation system was modeled for both summer and winter days' conditions.

A wide spectrum of studies can be found in the literature proposing geothermal driven CCHP. However, compared to the previously published literature [69,70], the proposed system demonstrated also a higher exergetic efficiency.

Absorption chiller and ORC were optimized regarding the generator temperature and evaporator pressure level, respectively. Under the optimized condition for these units, obtained results proved that a second law efficiency of almost 60% is reachable for the proposed domestic-scaled CCHP, while almost all of the geothermal fluid is utilized for domestic cooling and hot water production (no power production). Through numerous case studies, the most exergy destructive components were recognized, destruction within each main component was estimated and it was found that, under the base condition, Gen and ORCE are the most exergy destructive components with 24 and 21% of entire exergy destruction within the system, respectively. It was also shown that increasing the ORC supply is not a good idea from the exergy efficiency point of view (unlike energy efficiency). However, it should be noticed that not only electricity is extremely more valued in most of the European energy markets, but also their heat sectors are to be occupied with efficient electricity-driven technologies, e.g. heat pumps. Therefore, employing an ORC to increase the share of electricity in the proposed geothermal-driven CCHP is highly recommended. In addition, based on the sensitivity analysis, it was observed that any changes in the geothermal source volumetric flow rate would not have any significant effect on the system sustainability and thermodynamic performance while increasing source temperature from 368 to 378 K could reduce the energy efficiency from 56.22 to 55.38%, the exergy efficiency from 51.74 to 48.01% and the sustainability index from 2.07 to 1.92.

Acknowledgment

This research is part of the "HeatReFlex-Green and Flexible Heating/Cooling" project (www.heatreflex.et.aau.dk) funded by Danida Fellowship Centre and the Ministry of Foreign Affairs of Denmark under the grant no. 18-M06-AAU.

Nomenclature

Abbreviations

Abs	absorber
COND	condenser
Eva	evaporator

Gen	generator
HE	heat exchanger
HW	hot water
ORCC	ORC unit condenser
ORCE	ORC unit evaporator
ORCP	ORC unit pump
ORCT	ORC unit turbine
P	pump
SHE	solution heat exchanger
SPC	space cooling
SPH	space heating

Latin letters

e	specific physical exergy (kJ/kg)
eff	effectiveness
$\dot{E}$	exergy flow rate (kW)
h	specific enthalpy (J/kg)
$\dot{m}$	mass flow rate (kg/s)
$\dot{Q}$	heat transfer rate (kW)
R	gas constant (kJ/kg K)
s	entropy (kJ/kg K)
T	temperature (K)
$\dot{W}$	power (kW)

Greek letters

η	energy efficiency (-)
ε	exergy efficiency (-)

Subscripts

ch	chemical
D	destruction
e	outlet
i	inlet
is	isentropic
$ORCG$	ORC unit generator
ph	physical
t	overall
0	ambient conditions

References

[1] A. Hepbasli, A review on energetic, exergetic and exergoeconomic aspects of geothermal district heating systems (GDHSs), Energy Convers. Manag. 51 (2010) 2041–2061. https://doi.org/10.1016/J.ENCONMAN.2010.02.038.

[2] M. Yürüsoy, A. Keçebaş, Advanced exergo-environmental analyses and assessments of a real district heating system with geothermal energy, Appl. Therm. Eng. 113 (2017) 449–459.

https://doi.org/10.1016/J.APPLTHERMALENG.2016.11.054.

[3] S. Simsek, NEW WIDE DEVELOPMENT OF GEOTHERMAL POWER PRODUCTION IN TURKEY, in: Int. Geotherm. Days Slovakia, 2009. https://pangea.stanford.edu/ERE/pdf/IGAstandard/ISS/2009Slovakia/I.4.SIMSEK.pdf.

[4] M.F. Şener, A. Baba, Geochemical and hydrogeochemical characteristics and evolution of Kozaklı geothermal fluids, Central Anatolia, Turkey, Geothermics. 80 (2019) 69–77. https://doi.org/10.1016/J.GEOTHERMICS.2019.02.012.

[5] M.S. Kırlı, M. Fahrioğlu, Sustainable development of Turkey: Deployment of geothermal resources for carbon capture, utilization, and storage, Energy Sources, Part A Recover. Util. Environ. Eff. 41 (2019) 1739–1751. https://doi.org/10.1080/15567036.2018.1549149.

[6] F.S. Tut Haklıdır, T. Özen Balaban, A review of mineral precipitation and effective scale inhibition methods at geothermal power plants in West Anatolia (Turkey), Geothermics. 80 (2019) 103–118. https://doi.org/10.1016/J.GEOTHERMICS.2019.02.013.

[7] V.M. Ambriz-Díaz, C. Rubio-Maya, E. Ruiz-Casanova, J. Martínez-Patiño, E. Pastor-Martínez, Advanced exergy and exergoeconomic analysis for a polygeneration plant operating in geothermal cascade, Energy Convers. Manag. 203 (2020) 112227. https://doi.org/10.1016/j.enconman.2019.112227.

[8] M. Soltani, F. Moradi Kashkooli, A.R. Dehghani-Sanij, A. Nokhosteen, A. Ahmadi-Joughi, K. Gharali, S.B. Mahbaz, M.B. Dusseault, A comprehensive review of geothermal energy evolution and development, Int. J. Green Energy. 16 (2019) 971–1009. https://doi.org/10.1080/15435075.2019.1650047.

[9] S.M. Alirahmi, S. Rahmani Dabbagh, P. Ahmadi, S. Wongwises, Multi-objective design optimization of a multi-generation energy system based on geothermal and solar energy, Energy Convers. Manag. 205 (2020) 112426. https://doi.org/10.1016/j.enconman.2019.112426.

[10] M. Soltani, F. M. Kashkooli, A.R. Dehghani-Sanij, A.R. Kazemi, N. Bordbar, M.J. Farshchi, M. Elmi, K. Gharali, M. B. Dusseault, A comprehensive study of geothermal heating and cooling systems, Sustain. Cities Soc. 44 (2019) 793–818. https://doi.org/10.1016/j.scs.2018.09.036.

[11] T.A.H. Ratlamwala, S. Waseem, Y. Salman, A.A. Bham, Geothermal and solar energy-based multigeneration system for a district, Int. J. Energy Res. (2019). https://doi.org/10.1002/er.4480.

[12] F. Sun, X. Zhao, X. Chen, L. Fu, L. Liu, New configurations of district heating system based on natural gas and deep geothermal energy for higher energy efficiency in northern China, Appl. Therm. Eng. 151 (2019) 439–450. https://doi.org/10.1016/J.APPLTHERMALENG.2019.02.043.

[13] M.S. Kırlı, M. Fahrioğlu, Sustainable development of Turkey: Deployment of geothermal resources for carbon capture, utilization, and storage, Energy Sources, Part A Recover. Util. Environ. Eff. 41 (2019) 1739–1751. https://doi.org/10.1080/15567036.2018.1549149.

[14] F. Marty, S. Serra, S. Sochard, J.-M. Reneaume, Simultaneous optimization of the district heating network topology and the Organic Rankine Cycle sizing of a geothermal plant, Energy. 159 (2018) 1060–1074. https://doi.org/10.1016/J.ENERGY.2018.05.110.

[15] M. Unverdi, Y. Cerci, Thermodynamic analysis and performance improvement of Irem geothermal power plant in Turkey: A case study of organic Rankine cycle, Environ. Prog. Sustain. Energy. 37 (2018) 1523–1539. https://doi.org/10.1002/ep.12818.

[16] H. Arat, O. Arslan, Exergoeconomic analysis of district heating system boosted by the geothermal heat pump, Energy. 119 (2017) 1159–1170. https://doi.org/10.1016/J.ENERGY.2016.11.073.

[17] M. Yürüsoy, A. Keçebaş, Advanced exergo-environmental analyses and assessments of a real district heating system with geothermal energy, Appl. Therm. Eng. 113 (2017) 449–459. https://doi.org/10.1016/J.APPLTHERMALENG.2016.11.054.

[18] N. Yamankaradeniz, Thermodynamic performance assessments of a district heating system with geothermal by using advanced exergy analysis, Renew. Energy. 85 (2016) 965–972. https://doi.org/10.1016/J.RENENE.2015.07.035.

[19] H. Kivanc Ates, U. Serpen, Power plant selection for medium to high enthalpy geothermal resources of Turkey, Energy. 102 (2016) 287–301. https://doi.org/10.1016/J.ENERGY.2016.02.069.

[20] A. Arabkoohsar, G.B. Andresen, Supporting district heating and cooling networks with a bifunctional solar assisted absorption chiller, Energy Convers. Manag. 148 (2017) 184–196. https://doi.org/10.1016/J.ENCONMAN.2017.06.004.

[21] A. Hepbasli, C. Canakci, Geothermal district heating applications in Turkey: a case study of Izmir–Balcova, Energy Convers. Manag. 44 (2003) 1285–1301. https://doi.org/10.1016/S0196-8904(02)00121-8.

[22] M. Jiménez-Arreola, C. Wieland, A. Romagnoli, Direct vs indirect evaporation in Organic Rankine Cycle (ORC) systems: A comparison of the dynamic behavior for waste heat recovery of engine exhaust, Appl. Energy. 242 (2019) 439–452. https://doi.org/10.1016/j.apenergy.2019.03.011.

[23] L. Talluri, D. Fiaschi, G. Neri, L. Ciappi, Design and optimization of a Tesla turbine for ORC applications, Appl. Energy. 226 (2018) 300–319. https://doi.org/10.1016/j.apenergy.2018.05.057.

[24] M. Jiménez-Arreola, R. Pili, C. Wieland, A. Romagnoli, Analysis and comparison of dynamic behavior of heat exchangers for direct evaporation in ORC waste heat recovery applications from

fluctuating sources, Appl. Energy. 216 (2018) 724–740. https://doi.org/10.1016/j.apenergy.2018.01.085.

[25] J. Freeman, K. Hellgardt, C.N. Markides, Working fluid selection and electrical performance optimisation of a domestic solar-ORC combined heat and power system for year-round operation in the UK, Appl. Energy. 186 (2017) 291–303. https://doi.org/10.1016/j.apenergy.2016.04.041.

[26] D.F. Dominković, K.A. Bin Abdul Rashid, A. Romagnoli, A.S. Pedersen, K.C. Leong, G. Krajačić, N. Duić, Potential of district cooling in hot and humid climates, Appl. Energy. 208 (2017) 49–61. https://doi.org/10.1016/j.apenergy.2017.09.052.

[27] M. Yari, Exergetic analysis of various types of geothermal power plants, Renew. Energy. 35 (2010) 112–121. https://doi.org/10.1016/j.renene.2009.07.023.

[28] H. Nami, F. Ranjbar, M. Yari, Methanol synthesis from renewable H2 and captured CO2 from S-Graz cycle – Energy, exergy, exergoeconomic and exergoenvironmental (4E) analysis, Int. J. Hydrogen Energy. 44 (2019) 26128–26147. https://doi.org/10.1016/J.IJHYDENE.2019.08.079.

[29] H. Nami, F. Ranjbar, M. Yari, Thermodynamic assessment of zero-emission power, hydrogen and methanol production using captured CO 2 from S-Graz oxy-fuel cycle and renewable hydrogen, Energy Convers. Manag. 161 (2018) 53–65.

[30] A.A. H. Nami, Improving the Power Share of Waste-Driven CHP Plants via Parallelization with a Small-Scale Rankine Cycle, a Thermodynamic Analysis, Energy. In Press (2019).

[31] A. Arabkoohsar, Non-uniform temperature district heating system with decentralized heat pumps and standalone storage tanks, Energy. 170 (2019) 931–941. https://doi.org/10.1016/J.ENERGY.2018.12.209.

[32] H. Athari, S. Soltani, M.A. Rosen, S.M. Seyed Mahmoudi, T. Morosuk, Gas turbine steam injection and combined power cycles using fog inlet cooling and biomass fuel: A thermodynamic assessment, Renew. Energy. 92 (2016) 95–103. https://doi.org/10.1016/j.renene.2016.01.097.

[33] A.R. Razmi, M. Janbaz, Exergoeconomic assessment with reliability consideration of a green cogeneration system based on compressed air energy storage (CAES), Energy Convers. Manag. 204 (2020). https://doi.org/10.1016/j.enconman.2019.112320.

[34] J. Sarkar, Second law analysis of supercritical CO2 recompression Brayton cycle, Energy. 34 (2009) 1172–1178. https://doi.org/10.1016/j.energy.2009.04.030.

[35] M.M.K. Bhuiya, J.U. Ahamed, M.A.R. Sarkar, B. Salam, A.S.M. Sayem, A. Rahman, Performance of turbulent flow heat transfer through a tube with perforated strip inserts, Heat Transf. Eng. 35 (2014) 43–52. https://doi.org/10.1080/01457632.2013.810449.

[36] A. Bejan, G. Tsatsaronis, Thermal design and optimization, John Wiley & Sons, 1996.

[37] S.M.S. Mahmoudi, M. Akbari Kordlar, A new flexible geothermal based cogeneration system producing power and refrigeration, Renew. Energy. 123 (2018) 499–512. https://doi.org/10.1016/j.renene.2018.02.060.

[38] A. Colmenar-Santos, G. Zarzuelo-Puch, D. Borge-Diez, C. García-Diéguez, Thermodynamic and exergoeconomic analysis of energy recovery system of biogas from a wastewater treatment plant and use in a Stirling engine, Renew. Energy. 88 (2016) 171–184. https://doi.org/10.1016/j.renene.2015.11.001.

[39] I. Dincer, Y.A. Cengel, Energy, entropy and exergy concepts and their roles in thermal engineering, Entropy. 3 (2001) 116–149.

[40] A. Nemati, M. Sadeghi, M. Yari, Exergoeconomic analysis and multi-objective optimization of a marine engine waste heat driven RO desalination system integrated with an organic Rankine cycle using zeotropic working fl uid, Desalination. 422 (2017) 113–123. https://doi.org/10.1016/j.desal.2017.08.012.

[41] T.J. Kotas, The exergy method of thermal plant analysis, 1st ed., Butterworths, London, 1998.

[42] J. Sargut, D.R. Morris, F.R. Steward, Exergy Analysis of Thermal, Chemical, and Metallurgical Processes, Hemisphere Pub, Philadelphia, 1988.

[43] V. Zare, M. Yari, S.M.S. Mahmoudi, Proposal and analysis of a new combined cogeneration system based on the GT-MHR cycle, Desalination. 286 (2012) 417–428.

[44] Y. Luo, X. Wu, Y. Shi, A.F. Ghoniem, N. Cai, Exergy analysis of an integrated solid oxide electrolysis cell-methanation reactor for renewable energy storage, Appl. Energy. 215 (2018) 371–383. https://doi.org/10.1016/j.apenergy.2018.02.022.

[45] A. Razmi, M. Soltani, F. M. Kashkooli, L. Garousi Farshi, Energy and exergy analysis of an environmentally-friendly hybrid absorption/recompression refrigeration system, Energy Convers. Manag. 164 (2018) 59–69. https://doi.org/10.1016/j.enconman.2018.02.084.

[46] A. Razmi, M. Soltani, M. Torabi, Investigation of an efficient and environmentally-friendly CCHP system based on CAES, ORC and compression-absorption refrigeration cycle: Energy and exergy analysis, Energy Convers. Manag. 195 (2019) 1199–1211. https://doi.org/10.1016/j.enconman.2019.05.065.

[47] A. Razmi, M. Soltani, M. Tayefeh, M. Torabi, M.B. Dusseault, Thermodynamic analysis of compressed air energy storage (CAES) hybridized with a multi-effect desalination (MED) system, Energy Convers. Manag. 199 (2019). https://doi.org/10.1016/j.enconman.2019.112047.

[48] A. Razmi, M. Soltani, C. Aghanajafi, M. Torabi, Thermodynamic and economic investigation of a novel integration of the absorption-recompression refrigeration system with compressed air energy storage (CAES), Energy Convers. Manag. 187 (2019) 262–273. https://doi.org/10.1016/j.enconman.2019.03.010.

[49] S.M. Babaei, A.R. Razmi, M. Soltani, J. Nathwani, Quantifying the effect of nanoparticles addition to a hybrid absorption/recompression refrigeration cycle, J. Clean. Prod. 260 (2020) 121084. https://doi.org/10.1016/j.jclepro.2020.121084.

[50] H. Nami, A. Anvari-Moghaddam, Small-scale CCHP systems for waste heat recovery from cement plants: Thermodynamic, sustainability and economic implications, Energy. (2020) 116634. https://doi.org/10.1016/J.ENERGY.2019.116634.

[51] H. Nami, A. Arabkoohsar, A. Anvari-Moghaddam, Thermodynamic and sustainability analysis of a municipal waste-driven combined cooling, heating and power (CCHP) plant, Energy Convers. Manag. 201 (2019). https://doi.org/10.1016/j.enconman.2019.112158.

[52] K.W. Robert, T.M. Parris, A.A. Leiserowitz, What is Sustainable Development? Goals, Indicators, Values, and Practice, Environ. Sci. Policy Sustain. Dev. 47 (2012) 8–21. https://doi.org/10.1080/00139157.2005.10524444.

[53] I. Dincer, A.S. Joshi, Solar based hydrogen production systems, Springer, 2013.

[54] P. Ahmadi, I. Dincer, M.A. Rosen, Energy and exergy analyses of hydrogen production via solar-boosted ocean thermal energy conversion and PEM electrolysis, Int. J. Hydrogen Energy. 38 (2013) 1795–1805. https://doi.org/10.1016/J.IJHYDENE.2012.11.025.

[55] P. Ahmadi, I. Dincer, M.A. Rosen, Exergo-environmental analysis of an integrated organic Rankine cycle for trigeneration, Energy Convers. Manag. 64 (2012) 447–453. https://doi.org/10.1016/J.ENCONMAN.2012.06.001.

[56] H. Nami, S.M.S. Mahmoudi, A. Nemati, Exergy, economic and environmental impact assessment and optimization of a novel cogeneration system including a gas turbine, a supercritical CO2 and an organic Rankine cycle (GT-HRSG/SCO2), Appl. Therm. Eng. 110 (2017) 1315–1330.

[57] E. Akrami, A. Nemati, H. Nami, F. Ranjbar, Exergy and exergoeconomic assessment of hydrogen and cooling production from concentrated PVT equipped with PEM electrolyzer and LiBr-H2O absorption chiller, Int. J. Hydrogen Energy. 43 (2018) 622–633. https://doi.org/10.1016/j.ijhydene.2017.11.007.

[58] A. Arabkoohsar, M. Dremark-Larsen, R. Lorentzen, G.B. Andresen, Subcooled compressed air energy storage system for coproduction of heat, cooling and electricity, Appl. Energy. 205 (2017)

602–614. https://doi.org/10.1016/J.APENERGY.2017.08.006.

[59] A. Arabkoohsar, H. Nami, Thermodynamic and economic analyses of a hybrid waste-driven CHP–ORC plant with exhaust heat recovery, Energy Convers. Manag. 187 (2019) 512–522. https://doi.org/10.1016/j.enconman.2019.03.027.

[60] S.A. Klein, F.L. Alvarado, Engineering equation solver, (2002).

[61] N. Shokati, F. Ranjbar, M. Yari, Exergoeconomic analysis and optimization of basic, dual-pressure and dual-fluid ORCs and Kalina geothermal power plants: A comparative study, Renew. Energy. 83 (2015) 527–542. https://doi.org/10.1016/j.renene.2015.04.069.

[62] S.M. Alirahmi, S. Rahmani Dabbagh, P. Ahmadi, S. Wongwises, Multi-objective design optimization of a multi-generation energy system based on geothermal and solar energy, Energy Convers. Manag. 205 (2020) 112426. https://doi.org/10.1016/j.enconman.2019.112426.

[63] H. Nami, I.S. Ertesvåg, R. Agromayor, L. Riboldi, L.O. Nord, Gas turbine exhaust gas heat recovery by organic Rankine cycles (ORC) for offshore combined heat and power applications - Energy and exergy analysis, Energy. 165 (2018) 1060–1071. https://doi.org/10.1016/j.energy.2018.10.034.

[64] B.A. Younglove, M.O. Mclinden, An International Standard Equation of State for the Thermodynamic Properties of Refrigerant 123 (2,2-Dichloro-1,1,1-Trifluoroethane), J. Phys. Chem. Ref. Data. 23 (1994) 731–779. https://doi.org/10.1063/1.555950.

[65] F. Mohammadkhani, N. Shokati, S.M.S. Mahmoudi, M. Yari, M.A. Rosen, Exergoeconomic assessment and parametric study of a Gas Turbine-Modular Helium Reactor combined with two Organic Rankine Cycles, Energy. 65 (2014) 533–543.

[66] A. Mohammadi, M. Mehrpooya, Energy and exergy analyses of a combined desalination and CCHP system driven by geothermal energy, Appl. Therm. Eng. 116 (2017) 685–694. https://doi.org/10.1016/J.APPLTHERMALENG.2017.01.114.

[67] F.A. Boyaghchi, M. Chavoshi, Multi-criteria optimization of a micro solar-geothermal CCHP system applying water/CuO nanofluid based on exergy, exergoeconomic and exergoenvironmental concepts, Appl. Therm. Eng. 112 (2017) 660–675. https://doi.org/10.1016/J.APPLTHERMALENG.2016.10.139.

[68] A. Hepbasli, M.T. Balta, Z. Alsuhaibani, Comparing the Energetic and Exergetic Performances of a Building Heated by Solar Energy and Ground-Source (Geothermal) Heat Pump, Adv. Mater. Res. 347–353 (2011) 1801–1805. https://doi.org/10.4028/www.scientific.net/AMR.347-353.1801.

[69] V. Zare, H. Rostamnejad Takleh, Novel geothermal driven CCHP systems integrating ejector transcritical CO2 and Rankine cycles: Thermodynamic modeling and parametric study, Energy

Convers. Manag. 205 (2020) 112396. https://doi.org/10.1016/j.enconman.2019.112396.

[70] J. Wang, C. Ren, Y. Gao, H. Chen, J. Dong, Performance investigation of a new geothermal combined cooling, heating and power system, Energy Convers. Manag. 208 (2020) 112591. https://doi.org/10.1016/j.enconman.2020.112591.